Supporting Information

A Polarity-Sensitive Fluorescent Probe Based on Difluoroboron Derivative for Monitoring Variation of Lipid Droplets

Hui Wang[†, *], Lei Hu[†], Shuting Shen, Kun Yu, Yaxuan Wang

Department of Chemistry, Wannan Medical College, Wuhu 241002, People's Republic of China

† These authors contributed equally to this work and should be considered co-first authors.

E-mail address: wanghias@126.com (H. Wang)

Experimental section

Measurements and apparatus

All reagents were obtained commercially and used as supplied. Mass spectrum was obtained on HRMS-LTQ Obritrap XL (ESI source). ^{1}H-NMR and ^{13}C-NMR spectra were recorded on a Bruker Avance 400 spectrometer (TMS as internal standard in NMR). UV spectra were measured on a UV-5900 PC spectrophotometer. IR spectra were recorded on a Nicolet FT-IR-is5 spectrophotometer in the 4000-400 cm^{-1} range with samples prepared as KBr pellets. The fluorescence spectra were measured on a HITACHI F-4600 fluorescence spectrophotometer.

Synthesis of LD-L

Compound **1** 0.33 g (2.23 mmol, 1 eq.) was dissolved in 5 mL toluene, to which a solution containing 0.65 g (2.23 mmol, 1 eq.) compound **2** was dropwise added. Then 0.63 mL (2.5 mmol) tributyl borate and 0.1 mL n-butylamine were added. The mixture was stirred at 60 °C for 10 h. After cooling, the solvent was removed under vacuum suction. The coarse product was purified by column chromatography (petroleum ether/ethyl acetate, v/v= 5:1) to obtain red powder **LD-L** (0.41 g, Yield 43 %). IR (selected bands, KBr, cm^{-1}): 2986, 2939, 1742, 1624, 1598, 1544, 1502, 1447,

1348, 1299, 1267, 1185, 1185, 1169, 1061, 992, 970, 818. ^{1}H-NMR (400 MHz, d_6-Acetone, ppm) δ 8.01 (d, J = 15.5 Hz, 1 H), 7.71 (d, J = 9.0 Hz, 2 H), 6.83-6.70 (m, 3 H), 6.26 (s, 1 H), 4.36 (s, 4 H), 4.19 (q, J = 7.1 Hz, 4 H), 2.31 (d, J = 15.7 Hz, 3 H), 1.24 (t, J = 7.1 Hz, 6 H). ^{13}C-NMR (101 MHz, d_1 Chloroform) δ: 188.75, 180.81, 169.71, 151.25, 149.15, 131.77, 123.88, 115.14, 112.54, 100.79, 61.62, 53.33, 24.09, 14.22. ESI-MS [m/z-H]: Calculated, 423.220. Found, 422.263.

Computational details

The ground state geometries of **LD-L** are optimized at the time-dependent density functional theory (TD-DFT)/ B3LYP functional level without any symmetry restraint using Gaussian 09 program. The emission properties are obtained based on the optimized structures with B3LYP functional utilizing Gaussian 09 package. The basis set of 6-31G is chosen for all atoms. An analytical frequency confirms evidence that the calculated species represents a true minimum without imaginary frequencies on the respective potential energy surface. The molecular orbitals were visualized using GaussView 5.0.9.

The Lippert-Mataga equation is the most widely used equation to evaluate the dipole moment changes of the dyes with photoexcitation [1-2]:

$$\Delta v = \frac{2\Delta f}{4\pi\varepsilon_0 hca^3}(\mu_e - \mu_g)^2 + b$$

$$\Delta f = \frac{\varepsilon - 1}{2\varepsilon + 1} - \frac{n^2 - 1}{2n^2 + 1}$$

in which $\Delta v = v_{abs} - v_{em}$ stands for Stokes shift, v_{abs} and v_{em} are absorption and emission (cm^{-1}), h is the Planck's constant, c is the velocity of light in vacuum, a is the Onsager radius and b is a constant. Δf is the orientation polarizability, μ_e and μ_g are the dipole moments of the emissive and ground states, respectively and ε_0 is the permittivity of the vacuum. $(\mu_e - \mu_g)^2$ is proportional to the slope of the Lippert -Mataga plot.

Cell Imaging

HepG2 cells were seeded in 35 mm glass bottom plates at a density of 5×10^6 cells and grown for 48 hours. **LD-L** was first dissolved in DMSO to 1 mM as stock solution, and then diluted by DMEM cell culture medium to the working concentration (10 μM). For live cell imaging, cells were incubated with **LD-L** at 10 μM in cell medium containing 10 % FBS and maintained at 37 °C in an atmosphere of 5% CO_2 and 95% air for 1 h.

Cytotoxicity assays in cells

HepG2 cells were prepared for cell viability studies in 96-well plates at a density of 10^5 cells/well. Cells were grown to ~85% confluence in 96-well plates before treatment. **LD-L** was then added at indicted concentrations to triplicate wells. Prior to the compound' treatment, cell culture medium was changed, and aliquots of the compounds stock solutions were diluted to obtain the final concentrations. After incubation for 24 h, the medium was replaced with fresh DMEM medium. Subsequently, cells were treated with 5 mg/mL MTT (10 μL/well) and incubated for an additional 4 h (37 °C, 5% CO_2). After MTT medium removal, the formazan crystals were dissolved in DMSO (100 μL/well) and the absorbance was measured at 490 nm using a microplate reader (Infinite 2000pro).

Photostability test

In order to test the photostability of **LD-L** and HCS Lipid TOX Deep Red in cells, live probe-labelled HepG2 cells were imaged on a confocal microscope using Leica TCS SP8 under the same laser power. Confocal fluorescence images were collected every 30 s in the channel. Conditions: for **LD-L**, excitation wavelength: 488 nm and emission filter: 510-560 nm; for HCS Lipid TOX Deep Red, excitation wavelength: 633 nm and emission filter: 645-675 nm.

Animal experiment

All procedures involving animals were approved by and conformed to the guidelines of the Wannan Medical College. We have taken great efforts to reduce the

number of animal used in these studies and also taken effort to reduce animal suffering from pain and discomfort.

Tissue Section

For the fixed mouse brain slice, the mouse brain was isolated from their skulls and put into 4 % paraformaldehyde for 4 days then dehydrated in 30 % sucrose solution. For the fresh mouse brain tissue, separated fresh brain was put in liquid nitrogen surrounding by isopentane. The fixed and fresh mouse brain slices (30 μm) were obtained by Leica CM3050S freezing microtome. The slices were stained with **LD-L** (10 μM) for 1 h at 37 °C. The imaging was performed after the slices were washed by PBS 3 times.
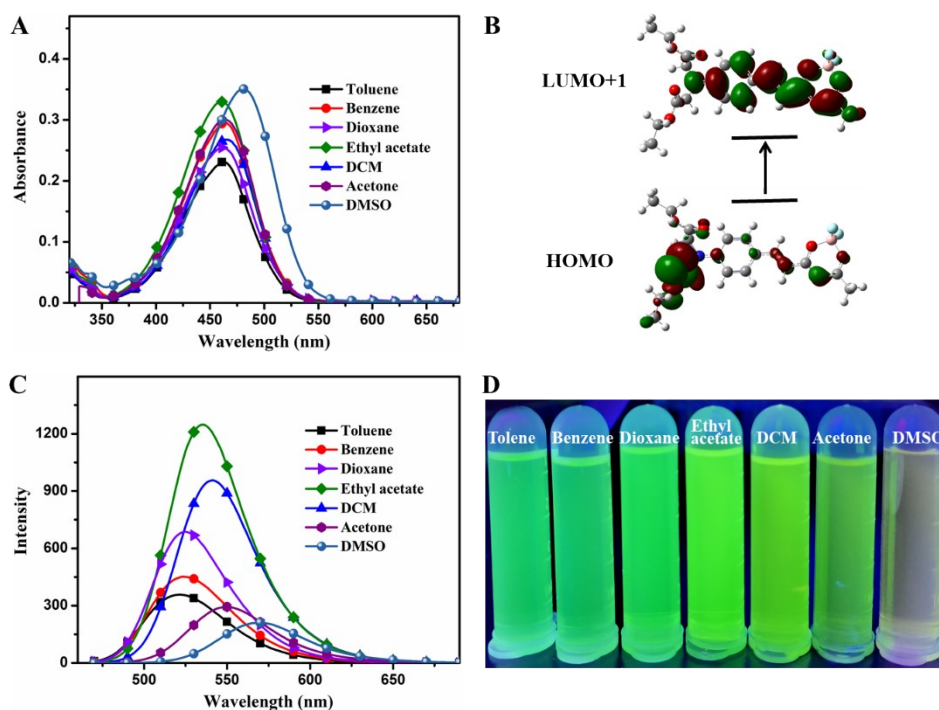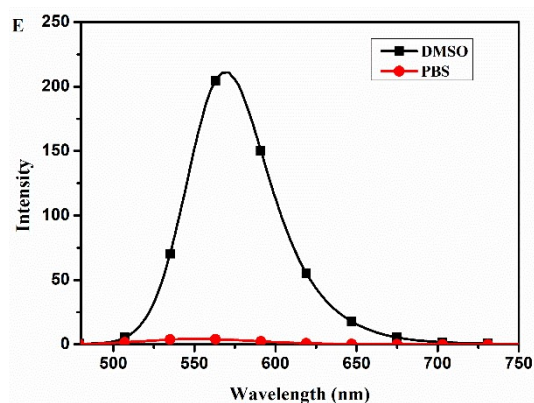
Figure S1. (A) Absorption spectra and (C) fluorescence spectra (λ_{ex} = 460 nm) of **LD-L** (10 μM) in different solvents. (B) Molecular orbital energy diagrams. (D) The photograph images for compound **LD-L** in different solvents under UV light (λ=365 nm). (E) Fluorescence spectra of **LD-L** (10 μM) in DMSO and PBS buffer solutions, respectively.
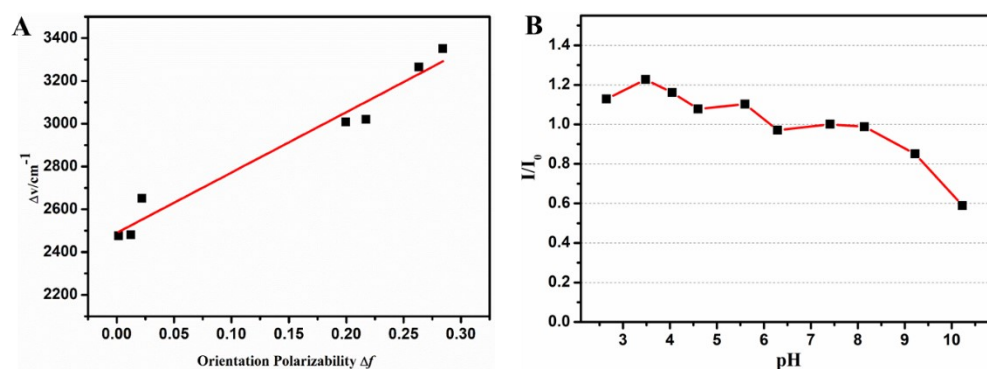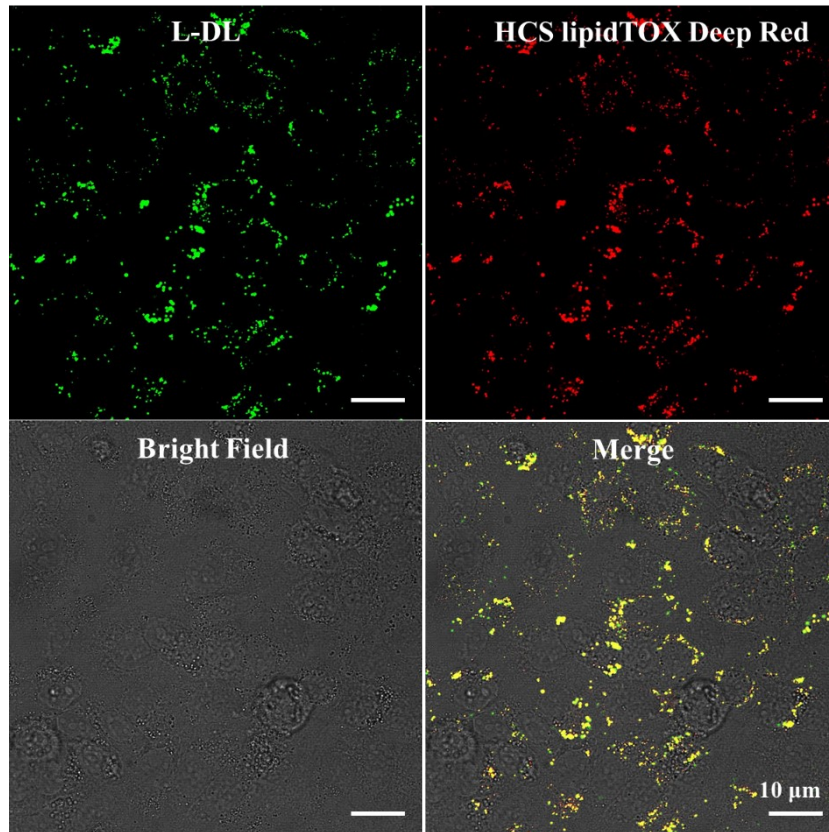

Figure S2. (A) Lippert-Mataga plots for compound **LD-L** (slope=2820.12). (B) Fluorescence intensity of **LD-L** in PBS buffer at various pH values (λ_{ex} = 460 nm).
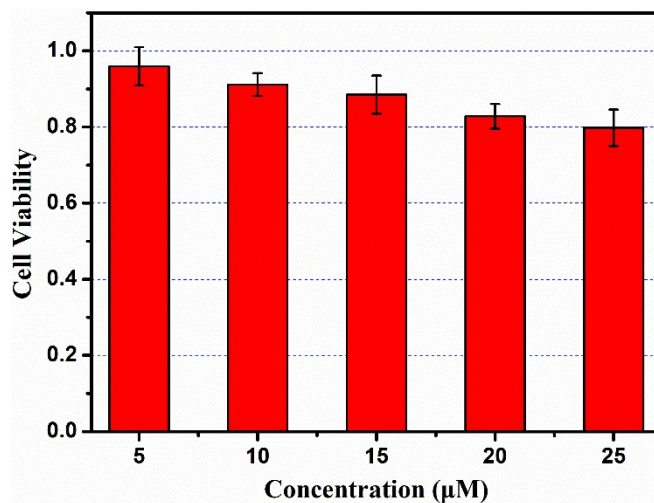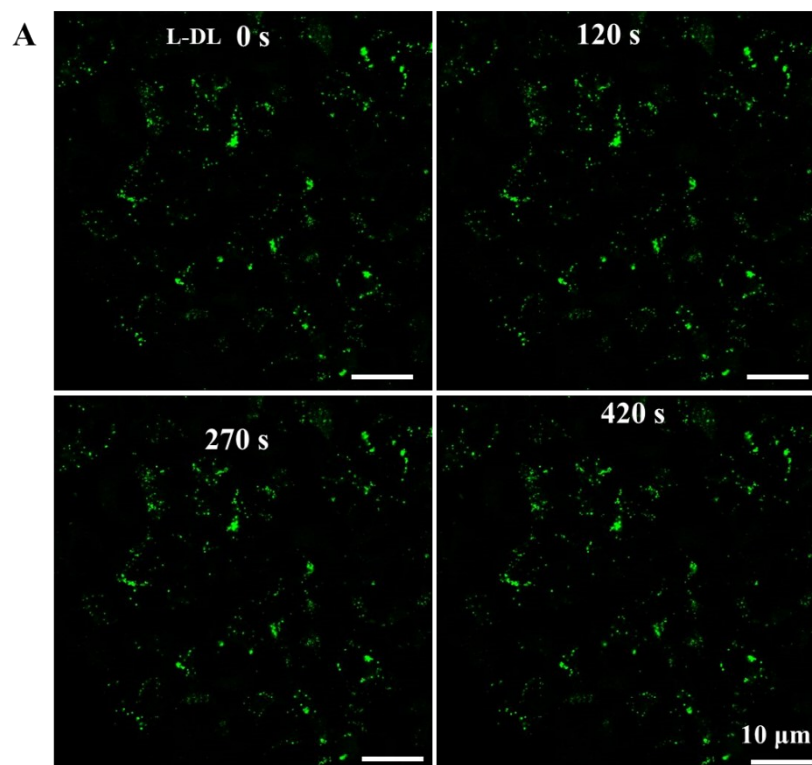
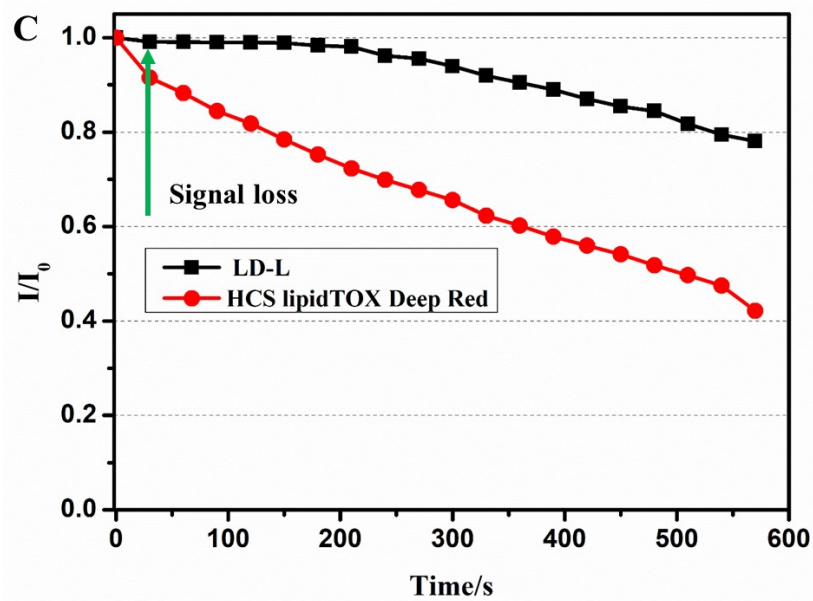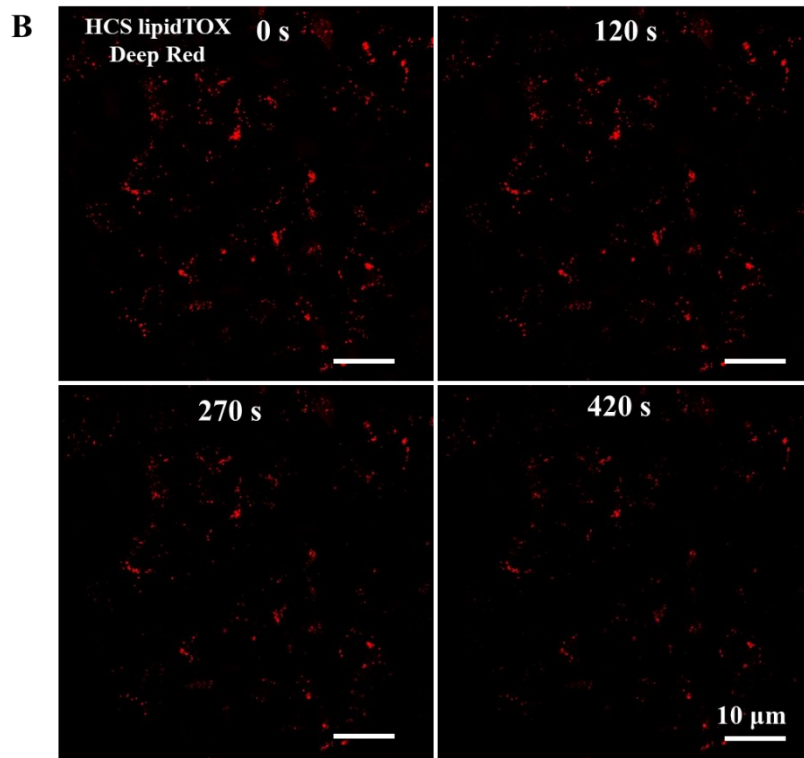**Figure S3.** MTT assay of living HepG2 cells after treated with **LD-L** for 24 h.
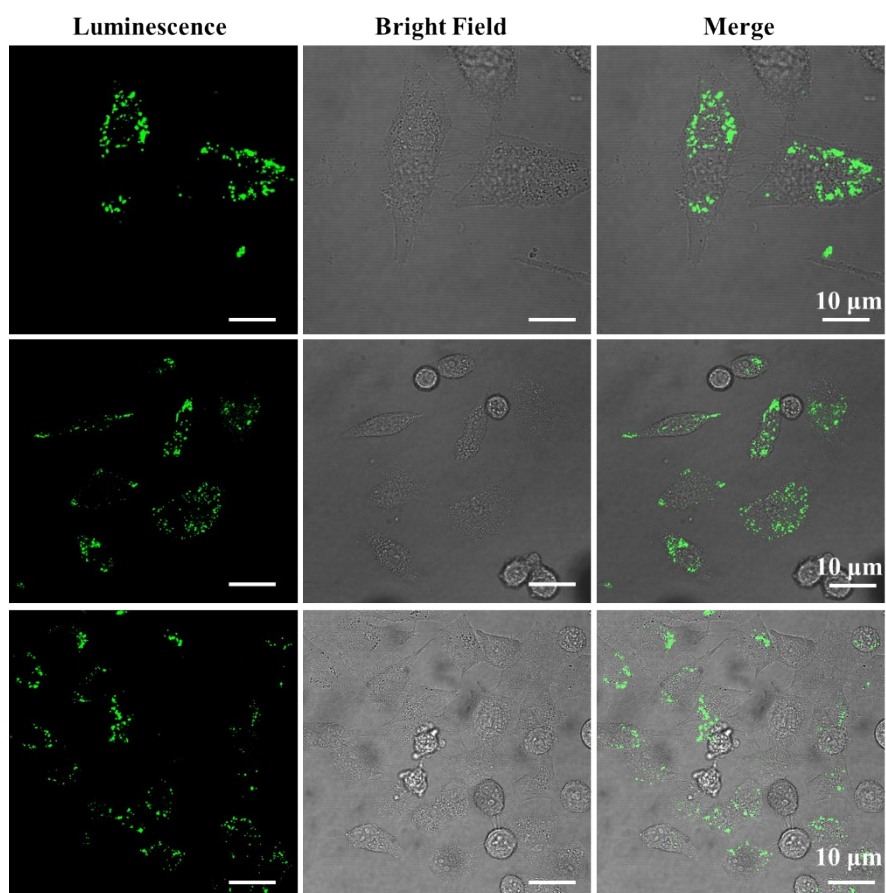
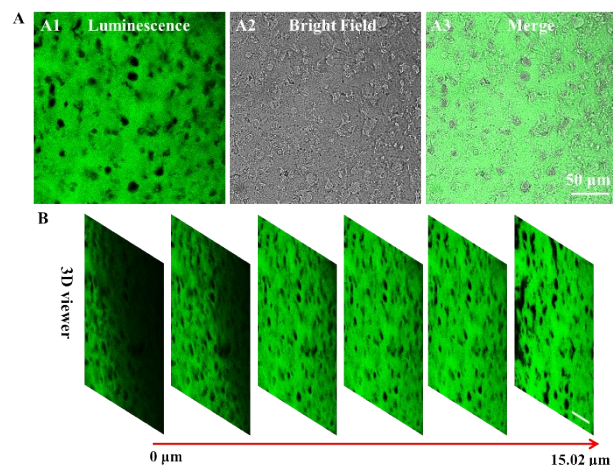**Figure S4.** Confocal images of living HepG2 cells stained with **LD-L** (λ_{ex} = 488 nm, λ_{em} = 510−560 nm). Scar bar = 10 μm.

Figure S5. Colocalization images of living HepG2 cells stained with **LD-L** (λ_{ex} = 488 nm, λ_{em} = 510-560 nm) and HCS Lipid TOX Deep Red (λ_{ex} = 633 nm, λ_{em} = 645-675nm), respectively. Scar bar = 10 μm.

Figure S6. Fluorescence imaging of **LD-L** (A) (λ_{ex} = 488 nm, λ_{em} = 510-560 nm) and HCS lipid TOX Deep Red (B) (λ_{ex} = 633 nm, λ_{em} = 645-675nm) under the ceaseless laser exposure, respectively. (C) Relative intensity loss of fluorescence emission of **LD-L** and HCS Lipid TOX Deep Red with an increasing bleaching time. (I_0 represents the initial intensity, I represents the intensity under the ceaseless laser exposure).

Figure S7. (A) Confocal images of living mouse brain sections treated with LD-L (10 μM) for 1 h (λex = 488 nm, λem = 510−560 nm). (B) The 3D reconstructed image of the brain sections. Scar bar = 50 μm.

Table S1. The photophysical data of **LDL** in different solvents.

| Solvents	λ^{abs}_{max} (nm)[a]	ε^{b}_{max}	λ^{SPEF}_{max} (nm)[c]	$\Delta\nu$ (nm)[d]	Φ[e]
Toluene	460	2.34	519	59	0.11
Benzene	462	2.99	524	62	0.10
Dioxane	461	2.58	525	64	0.18
Ethyl acetate	469	3.33	535	66	0.26
DCM	464	2.68	541	77	0.25
Acetone	463	3.02	549	86	0.07
DMSO	481	3.51	570	89	0.04
PBS	461	1.22	551	90	0.003

[a] Peak position of the longest absorption band. [b] Molar absorbance in 10^4 mol^{-1} L cm^{-1}. [c] Peak position of single-photon excited fluorescence (SPEF) spectra, excited at the absorption maximum. [d] Stokes' shift in nm. [e] Quantum yields determined by using fluorescein as standard.

Table S2 The critical comparison with the performance of known LDs-fluorescent probes.
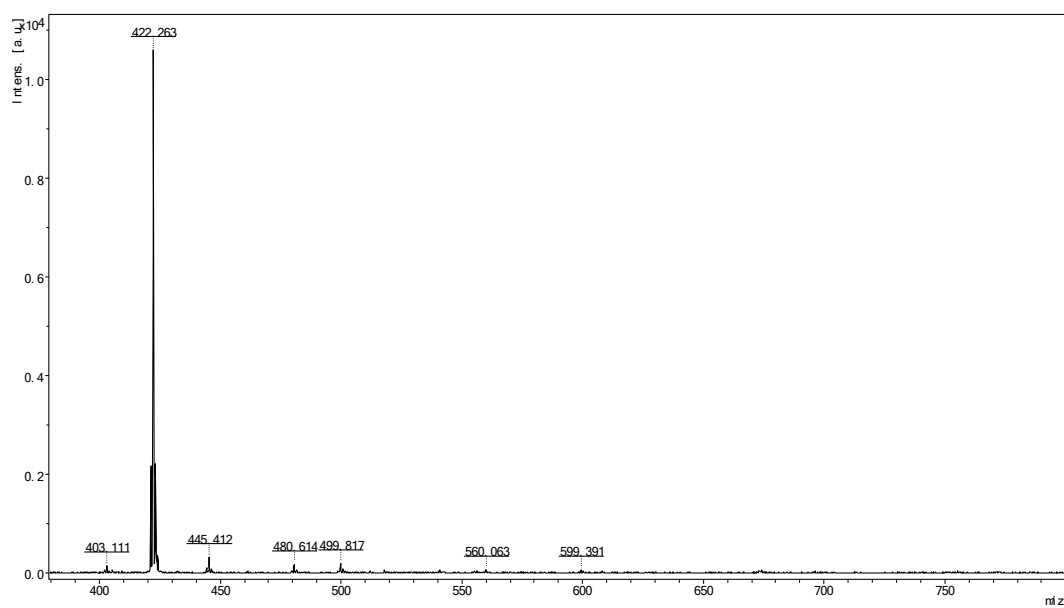
Probe name	Response to polarity	Mechanism study	References
LD-TTP	yes	no	[3]
CQPP	yes	no	[4]
DAF	yes	no	[5]
CM2P	no	yes	[6]
TPA-LD	no	yes	[7]
CCB	yes	no	[8]
CTPA	yes	no	[9]
CTPE	yes	no	[10]
CBA	no	no	[11]
L3	no	yes	[12]
FB	no	no	[13]
LD-L	yes	yes	**This work**
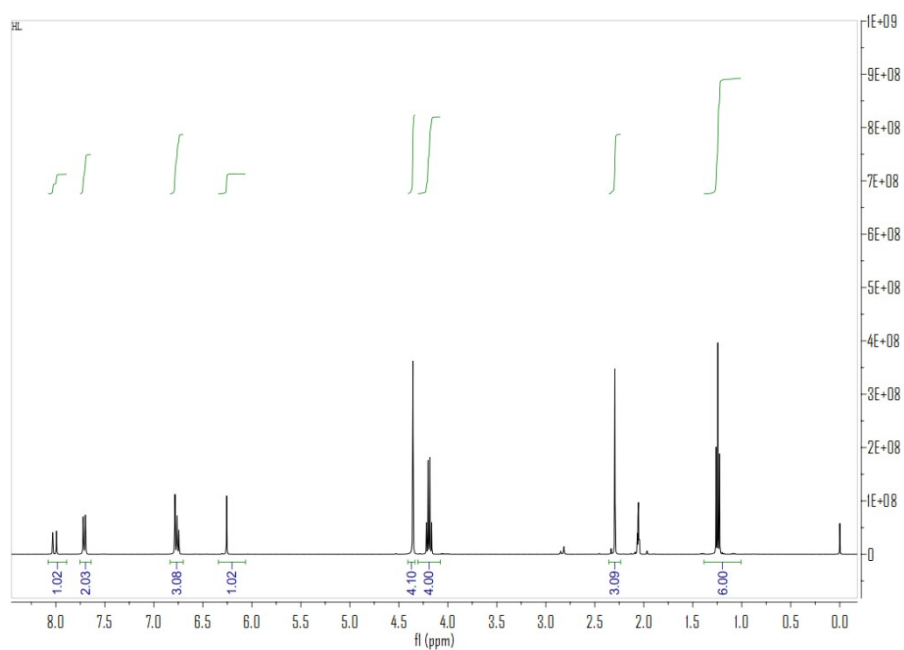
Figure S8. ^{1}H NMR spectra of **LD-L**.
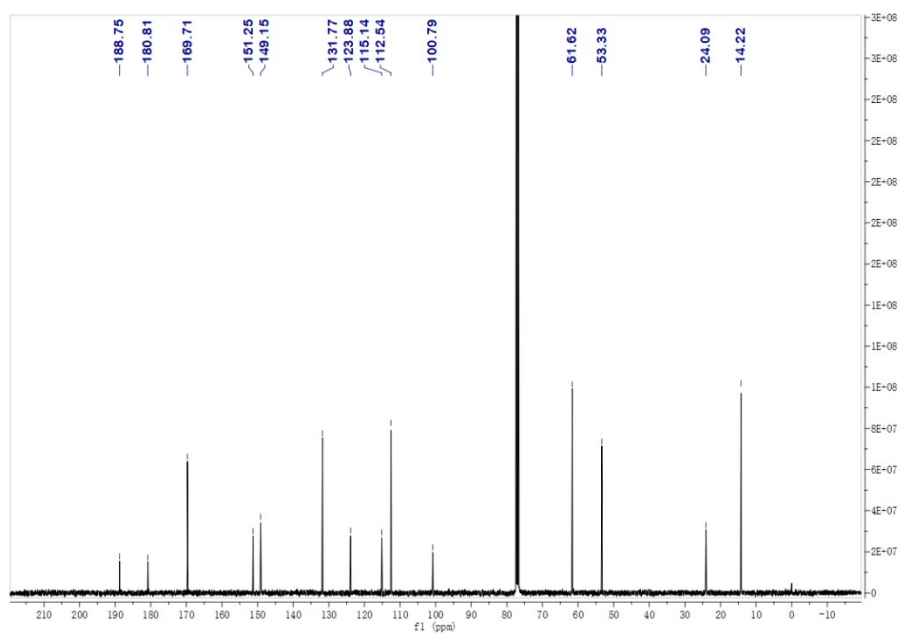
Figure S9. ^{13}C NMR spectra of **LD-L**.

Figure S10. MS spectra of **LD-L**.

References:

[1] S.A. Patel, M. Cozzuol, J.M. Hales, C.I. Richards, M. Sartin, J.C. Hsiang, T. Vosch, J.W. Perry, R.M. Dickson. J. Phys. Chem., 2009, 113, 20264-20270.

[2] S.M. Ji, J. Yang, Q. Yang, S.S. Liu, M.D. Chen, J.Z. Zhao. J. Org. Chem., 2009, 74, 4855-4865.

[3] L. Fan, X.D. Wang, Q. Zan, L.F. Fan, F. Li, Y.M. Yang, C.H. Zhang, S.M. Shuang, C. Dong. Anal. Chem., 2021, 93, 8019-8026.

[4] K.K. Wang, L.Y. Liu, D. Mao, S. D. Xu, C.P. Tan, Q. Cao, Z.W. Mao, B. Liu. Angew. Chem. Inter. Ed., 2021, 25, 15095-15100.

[5] M. Collot, S. Bou, T.K. Fam, L. Richert, L. Danglot, A.S. Klymchenko. Anal. Chem., 2019, 91, 1928-1935.

[6] H.K. Xu, H.H. Zhang, G. Liu, L. Kong, X.J. Zhu, X.H. Tian, Z.P. Zhang, R.L. Zhang, Z.C. Wu, Y.P. Tian, H.P. Zhou. Anal. Chem., 2019, 91, 977-982.

[7] X. Zhang, L. Yuan, J.X. Jiang, J.W. Hu, A.D. Rietz, H.Z. Cao, R.L. Zhang, X.H. Tian, F.L. Zhang, Y.G. Ma, Z.P. Zhang, K. Uvdal, Z.J. Hu. Anal. Chem., 2020, 02, 3613-3619.

[8] B.L. Lu, J.L. Yin, C. Liu, W.Y. Lin. Spectrochim. Acta. A. Mol. Biomol. Spetcrosc., 2021, 262, 120149.

[9] J.L. Yin, M. Peng, Y.Y. Ma, R. Guo, W.Y. Lin. Chem. Commun., 2018, 54, 12093-12096.

[10] C. Liu, J.L. Yin, B.L. Lu, W.Y. Lin. New. J. Chem., 2021, 45, 4347-4353.

[11] M. Peng, J.L. Yin, W.Y. Lin. New. J. Chem., 2018, 42, 18521-18525.

[12] S.J. Zhang, Z.H. Yang, M. H. Li, Q. Zhang, X.H. Tian, D.D. Li, S.L. Li, J.Y. Wu, Y.P. Tian. Analyst, 2020, 145, 7941-7945.

[13] Y.X. Wang, Y.T. Qiu, A.Y. Sun, Y.B. Xion, H.Y. Tan, Y.Q. Shi, P. Yu, G. Roy, L. Zhang, J.W. Yan. Anal. Chim. Acta., 2020, 1133, 109-118.